

# Feasibility of a Biomechatronic EPP Upper Limb Prosthesis Controller

Efie Moutopoulou, Georgios A. Bertos, *Member IEEE-EMBS*, Anestis Mablekos-Alexiou, *Student Member IEEE* and Evangelos G. Papadopoulos, *\* Senior Member, IEEE*

**Abstract**— In this paper, we examine the feasibility of an implantable topology of a Biomechatronic Extended Physiological Proprioception (EPP) Upper Limb Prosthesis Controller. Initial findings support the hypothesis that the topology is safe and feasible. This novel controller topology can maintain the advantages of EPP, but without its inherent disadvantages i.e. of the existence of unaesthetic cables, or mechanical linkages.

## I. INTRODUCTION

Prosthesis control schemes that employ the body's own actuating and sensing systems seem to be incorporated readily by prosthesis users. Such schemes may result in more subconscious control and position control than other control schemes [1]. Open-loop velocity control cannot provide this additional sensory feedback and does not result in more "subconscious control."

This phenomenon was first noted in 1974 by D.C. Simpson, who coined the term *Extended Physiological Proprioception* (EPP) to describe it [2]. EPP can best be thought of as the extension of the operator's proprioception into the prosthesis, that is, the prosthesis becomes an extension of the amputee's self [1]. The use of a tool such as a hammer illustrates the simplest form of EPP. We use the hammer as an extension of our hand; we extend our proprioception through it [3]. A conventional cable and harness operated body-powered arm is an example of good EPP control. Prosthesis state is available to the operator, via the tension in the control cable, at a subconscious level. The operator learns to equate shoulder position with that of the controlled prosthetic joint. Central to this concept of EPP is the idea that a prosthetic joint is physically linked to a physiological joint.

A traditional EPP controller has been implemented in previous works using the PIC16C73A Microchip microcontroller ([4], [5]). This microcontroller was used to drive a traditional EPP control scheme with a mechanical linkage (Bowden cable or harness) and an electronic force sensor for control input. The mechanical linkage exists and the electronic force sensor is driving the controller.

\* Research supported in part by the EU Marie Curie Integration Grant #334300. Georgios A. Bertos was previously with Northwestern University Prosthetics Research Laboratory, Chicago, IL, USA. Georgios A. Bertos, Efie Moutopoulou, Anestis Mablekos-Alexiou and Evangelos G. Papadopoulos are with the Department of Mechanical Engineering, Control Systems Laboratory, National Technical University of Athens (NTUA), Greece (phone: +30-210-772-3677, 1440; fax: +30-210-772-1450; e-mail: [george.bertos@gmail.com](mailto:george.bertos@gmail.com), [emoutopoulou@gmail.com](mailto:emoutopoulou@gmail.com), [mamplekos@gmail.com](mailto:mamplekos@gmail.com), [egpapado@central.ntua.gr](mailto:egpapado@central.ntua.gr)).

Therefore, the controller "assists" without sacrificing the inherent value of proprioception of EPP topology.

Nevertheless, this topology had the disadvantage of using unaesthetic for the amputee and the society Bowden cables and requires surgery after amputation. Our proposed topology does not include Bowden cables, and any necessary implant surgery is to be performed at the time of amputation; therefore the additional surgery disadvantage is also non-existent.

## II. PROPOSED ARCHITECTURE

In Figure 1. the proposed topology for the mechatronic EPP single degree-of-freedom (DOF) prosthesis model is presented. The commanding signal from an implanted force and position sensor is transmitted wirelessly to the controller and then to the dc-motor of the slave prosthesis, monitoring the prosthesis force, position and velocity.

As a feedback, another signal is transmitted back to the controller implanted into the hand, moving a micro dc-motor, connected to a tendon of the residual arm. In this way, the bidirectional communication of the master and slave controllers will result in the same feeling as in the case of using a Bowden cable.

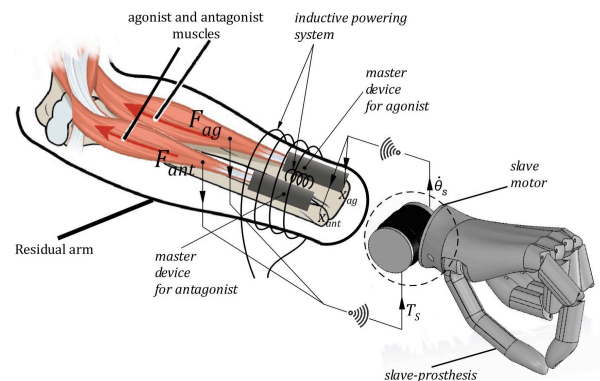


Figure 1. Basic concept of the mechatronic prosthetic hand. Two systems, the master device and its slave prosthesis, communicate bi-directionally, to provide a proprioceptive sensation.

### A. Master Device

The master device, implanted into the residual arm, consists of two 0.5 W DC motors connected to a tendon/muscle via a screw-nut system. A force sensor, a microcontroller, a wireless module, a battery and a wireless powering system are also part of the implanted system. All parts are selected

with the criteria of small size, low power consumption, high functionality and safety for human tissues.

Based on a comparison of the different options across meaningful criteria for the wireless communication, the Bluetooth Smart module PAN1740, characterized by very low power consumption of 4.9 mA was selected. Alternative options included RF, ZigBee and NFC, see Table I. The Bluetooth Smart module has the additional advantage of using a commercial product as opposed to a custom made application in the range of the Industrial Scientific Medical (ISM) bands (TABLE I. ).

As far as the wireless charging system, amongst the options of Inductive Coupling, RF and Ultrasound, Inductive Coupling was chosen, see TABLE II, due to its high efficiency and power transfer capability [6]. The basic concept of Inductive Coupling is illustrated in Fig. 2. For the purposes of our project, the primary circuit will be outside of the human hand, and the secondary circuit inside, charging the implanted battery (see Fig. 2).

TABLE I. WIRELESS CONNECTIONS

Parameters	Options			
	Bluetooth Smart SoC [7]	RF solutions [8]	NFC [9]	Zigbee [10]
Frequency	2.4 GHz	433 MHz	13.56 MHz	2.4 GHz
Human Safety	ISM band	safe	ISM band	ISM band
Power Consumption	R 4.9mA T 4.9mA	R 14.7mA T 15mA-30mA	>70mA	R 24mA T 29mA
Transmission Rates	~305Kbps	~250Kbps	106-848 Kbps	~250Mbps
Signal Range	>10m	>10 m	5-10 cm (-4 cm)	>10m
Size(mm x mm)	2.5 x 2.5	5 x 5	5 x 5	6 x 6

TABLE II. WIRELESS CHARGING OPTIONS

Parameters	Options		
	Inductive Coupling [11][12]	RF [6][13]	Ultrasound [14][12]
Human Safety	Depends on the energy transferred	Yes	Yes
Efficiency	73%	48%	21-35%
Max Power	Up to 10 W	< 1W	100 mW
Frequencies	1kHz-100 MHz	30 kHz - 300 GHz	10 kHz - 10 MHz

Primary Circuit

Secondary Circuit

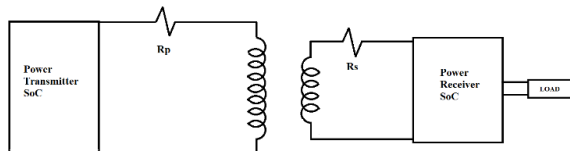


Figure 2. Wireless charging system based on inductive coupling [6]. We are using a power transmitter SoC connected to a coil on the primary circuit

and a combination of a coil and a power receiver SoC on the secondary circuit in order to charge the implanted battery.

### B. Slave System

The slave system consists of the prosthetic 1-DOF hand with a DC motor, microprocessor, Bluetooth Smart module and the powering system, see Fig. 1. All these components were chosen with the same criteria as the master system's components.

### III. CONSIDERATIONS

The major consideration about this system is human safety with respect to the aspects of wireless connection and wireless charging. When it comes to Bluetooth Smart, which operates in the range of 2.4 GHz frequencies, many studies have shown that there are no problems caused from the interaction with human tissues, since its operation is in the ISM bands. On the other hand, wireless powering needed more research in order to estimate the temperature rise, caused by the thermal losses in the hand, and to prevent tissue damage.

According to the efficiency of each element, we can estimate the power losses of our system. Each motor and screw-nut system has an efficiency of about 24%. This means that if this system needs 1 W of power, then 0.76 W will be thermal losses. Also we take into consideration the losses at the secondary coil of our wireless powering system. To power both of the motors, we need 2 W in the secondary coil. This means that with an efficiency of 70%, on the primary coil are needed 2.9 W and of those, 0.9W will be losses. The Bluetooth Smart SoC has a power consumption of 4.9 mW, which is negligible compared to the power mentioned previously.

In TABLE III, a summary of the required power values for the different subsystems and the estimated power losses, which lead to temperature rise into the hand's tissue, is presented.

TABLE III. POWER FLOW

Implant elements	Parameters		
	Efficiency	Power Needed	Losses
Bluetooth Smart SoC PAN1740	-	15.5 mW	<1 mW
Motor and Screw Nut System	24%	1W	0.76 W
Inductive Power System	70%	(on primary) 2.9 W	0.9 W

Assuming that the hand can be modeled as a multilayered-cylinder, so that we simplify our estimates for the temperature in each layer, an analysis of the heat transfer as it flows to the environment was performed, see Fig. 4.

To convert the multilayered-cylinder model into a thermal circuit, we will use the following equations:

$$Q = \frac{T_i - T_{i-1}}{R_i} \quad (1)$$

and

$$R_i = \frac{\ln\left(\frac{r_{i-1}}{r_i}\right)}{2\pi l k_i} \quad (2)$$

where  $Q$  is the heat flow,  $R_i$  is the thermal resistance of each layer,  $r_{i-1}$  is the corresponding outer radius of the layer,  $r_i$  is the corresponding inner radius of the layer,  $k_i$  is the layer thermal conductivity coefficient, and  $l$  is the length of the cylinder through which heat flows.

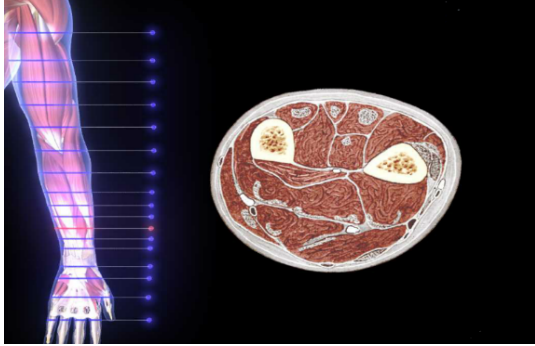


Figure 3. Cross Section of Antebrachium [16].

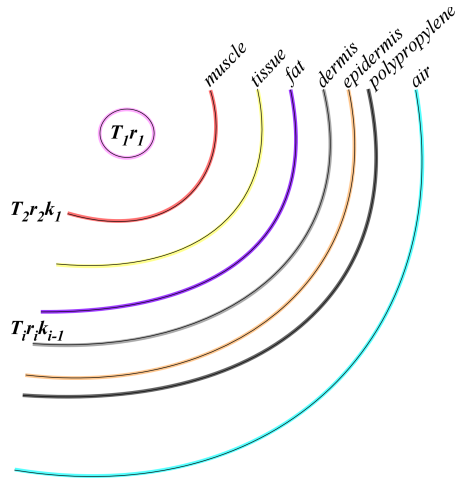


Figure 4. Cylindrical model of the hand and surrounding materials.

We assumed  $l$  to be  $3 * 10^{-2}$  m. We should note also, that for the heat transfer through the air layer we have heat convection characterized by its thermal resistance:

$$R = \frac{1}{hA} \quad (3)$$

where  $h$  is air's convection coefficient and  $A = 2\pi l r_s$ , with  $r_s$  the external radius of the hand.

Our model is simplified because our primary goal is to have an estimate for the temperature inside the arm in order to set the limits for the power of the system. We assumed that the heat flows radially even if in reality it flows also to the two bases of the cylinder, see Fig. 5. This means that the actual rise in the temperature will be lower than the estimated here.

The thickness of each layer was estimated, considering that the radius of an average hand is 29 mm, and the results are given in Table IV. With the help of this table, we can estimate the rise in temperature at the various layers of the hand. Indeed, all thermal resistances are calculated and are considered as a system of resistances due to conduction and convection connected in series. Using simple circuit analysis, one can find the temperature at each layer, as well as the total temperature drop from the center of the hand to its surface.

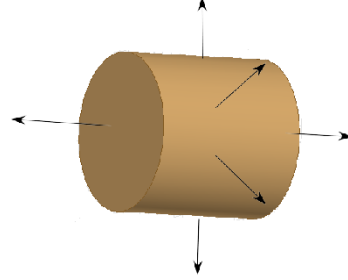


Figure 5. Heat flows in every direction.

TABLE IV. HUMAN HAND

Hand's Layer	Parameters	
	Thermal Conductivity (W/mK)	Thickness (mm)
§	-----	8.0
Muscle	0.530	16.1
Tissue & Blood (incl. Bone)	0.500	2.5
Fat	0.185	1.2
Dermis	0.400	1.1
Epidermis	0.235	0.1
Thermoplastic	0.250	1.0
Air (h)	10 (W/m <sup>2</sup> K)	20.0

#### IV. RESULTS

To minimize heat concentration, we assumed that the motors and the secondary circuit for the power are placed at different positions in the hand. As discussed previously, each motor-screw-nut system has losses of 0.76 W and the power system has losses of 0.9 W.

The losses of the inductive powering system come as result of the copper losses in the primary and secondary coils. This means that in the secondary coil, which is inside the human hand, we will have less than 0.9 W of thermal losses, despite the fact that in our analysis we take 0.9 W (worst condition) as datum.

In Figure 6, the temperature levels at each layer of the human hand are presented. The results were derived by the analysis described previously. In Fig. 6a, the temperature in

the region of the motor-screw-nut system is presented. The temperature in the region of the powering system is shown in Fig. 6b.

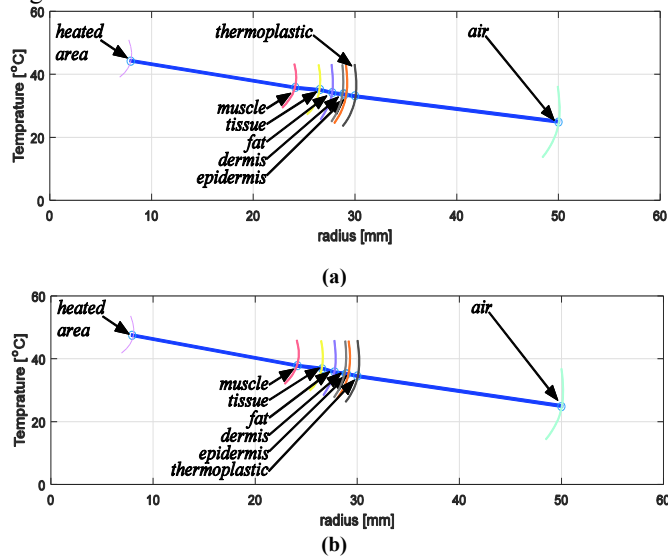


Figure 6. (a) Temperature level in each layer of the human hand in the region of: (a) motor-screw nut system, (b) powering system.

## V. DISCUSSION

The temperature rise into the hand's tissues is a basic limitation for the system design. Apart from the importance of a fully functional prosthesis, a basic parameter is our system's interaction with the human hand. Related studies [15] indicate that 44 °C is a critical threshold for the tissues. As shown in Figure 6, this requirement is satisfied by our component selection and overall design. Requirements for low power and less power losses may lead to a change of the initial topology.

As it seems, most of the power is consumed by the motors and screw-nut systems, which have low efficiency (around 24%). As in all prosthetic systems, it is apparent and in this case even more reinforced that there is a design trade-off between low power constraints and increased functionality.

Our system's feasibility is strongly connected to the design of the topology and the selection of the appropriate components. We are planning to implement this topology after these favorable feasibility studies in order to produce a working prototype. The system can be a functional, meaningful biomechatronic EPP-enhanced building block leading to many DOF prosthetic arms with superior control capabilities.

## VI. CONCLUSION

The topology and the feasibility of a novel Biomechatronic EPP equivalent upper limb prosthesis controller was presented. It consists of two basic subsystems, a master and a slave, which bi-directionally communicate with each other in order to provide an additional sensory feedback to the human hand – similar to the traditional EPP topology. Major

considerations include the size and the power of the motors and the electronics that will be used, and consequently the thermal losses and their effects to the human tissues. The proposed controller is shown to be safe, feasible and implementable; therefore the next step will be the implementation of a prototype. Vibrations caused by the dc-motors in the implant will be reduced by means of vibration isolation. This controller topology can function as a building block for additional DOF upper-limb prostheses, with the advantage of Extended Physiological Proprioception (EPP).

## VII. REFERENCES

- [1] R.F. ff. Weir and D.S. Childress, *Encyclopedia of Applied Physics*, vol. 15, 1996, pp.115-140.
- [2] Simpson, D.C., "The Choice of Control System for multimovement prostheses: Extended Physiological Proprioception (EPP)" in: *Control of Upper-Extremity Prostheses & Orthoses*, P. Herberts et al. (Eds), C.C. Thomas, 1974, pp. 146-150.
- [3] D.S. Childress, D.S., *Progress in Bioengineering*, Paul (Eds.), Adam Highler, pp. 210-215 1989.
- [4] Y.A. Bertos, "A Microprocessor-based EPP Position Controller for Electric-Powered Upper-Limb Prostheses", MS Thesis, Northwestern University, Evanston, IL, USA, 1999.
- [5] Y.A. Bertos, C.W. Heckathorne, R.F. ff. Weir and D.S. Childress, "Microprocessor Based E.P.P. Position Controller for Electric-Powered Upper-Limb Prostheses", *Proceedings of the 19th Annual Int. Conference of the IEEE-EMBS Society*, pp. 2311–2314 1997.
- [6] K. Van Schuylenbergh, *Inductive Powering-Basic theory and application to biomedical systems*
- [7] G. Description, "DA14580 Low Power Bluetooth Smart SoC DA14580," 2014.
- [8] Texas Instruments Inc., "TI Low Power RF Designer 's Guide to LPRF TI Low-Power RF at a glance ...," p. 64, 2010
- [9] G. Madlmayr, C. Kantner, and T. Grechenig, "Near Field Communication Texas Instruments," pp. 351–367, 2014.
- [10] Texas Instruments Inc., "A USB-Enabled System-On-Chip Solution for 2 . 4-GHz IEEE 802 . 15 . 4 and ZigBee Applications," no. September 2009, 2010.
- [11] S. Mutashar and M. Hannan, "Efficiency Improvement of Wireless Power Transmission for Bio-Implanted Devices," *Int. J. ...*, vol. 7, no. 12, pp. 721–724, 2013.
- [12] S. Ozeri and D. Shmilovitz, "Ultrasonic transcutaneous energy transfer for powering implanted devices," *Ultrasonics*, vol. 50, no. 6, pp. 556–566, 2010.
- [13] S. Senjuti, "Design and Optimization of Efficient Wireless Power Transfer Links for Implantable Biotelemetry Systems," *THESIS - U West. Ontario\_UWO*, p. 97, 2013
- [14] S. Arra, J. Leskinen, J. Heikkilä, and J. Vanhala, "Ultrasonic power and data link for wireless implantable applications," *2007 2nd Int. Symp. Wirel. Pervasive Comput.*, pp. 567–571, 2007
- [15] T. R. Gowrishankar, D. a Stewart, G. T. Martin, and J. C. Weaver, "Transport lattice models of heat transport in skin with spatially heterogeneous, temperature-dependent perfusion.," *Biomed. Eng. Online*, vol. 3, p. 42, 2004.
- [16] www.anatomyexpert.com